J Mater Sci (2016) 51:1428–1436
DOI 10.1007/s10853-015-9462-6

Synthesis of brush-like ZnO nanowires and their enhanced gas-sensing properties

Yongjiao Sun[1] · Zihan Wei[1] · Wendong Zhang[1] · Pengwei Li[1] · Kun Lian[1,2,3] · Jie Hu[1]

Received: 10 April 2015 / Accepted: 22 September 2015 / Published online: 19 October 2015

Abstract In this paper, brush-like ZnO nanowires were synthesized by two-step method combining electrospinning and hydrothermal. The phase purity, morphology, and structure of the brush-like ZnO hierarchical structures were characterized, which exhibited the improved surface area, comparing with ZnO nanofibers. The gas-sensing experiments were carried out on brush-like ZnO nanowires and ZnO nanofibers sensors under optimum working temperature. The highest response of brush-like ZnO nanowires to 100 ppm toluene and CO can reach to 12.7 and 5.9, respectively, which was much higher than that of ZnO nanofibers. Moreover, the brush-like ZnO nanowires sensor also shows fast response/recovery time to toluene (9/4 s) and CO (6/2 s), low detection limit (1 ppm to toluene). The measured results demonstrate that brush-like ZnO nanowires are potential as a novel sensing material for practical gas-sensing applications.

✉ Kun Lian
liankun@tyut.edu.cn

✉ Jie Hu
hujie@tyut.edu.cn

Yongjiao Sun
sunyongjiao0030@link.tyut.cn

Zihan Wei
weizihan0227@link.tyut.cn

Wendong Zhang
wdzhang@tyut.edu.cn

Pengwei Li
lipengwei@tyut.edu.cn

[1] Micro and Nano System Research Center, Information Engineering College, Taiyuan University of Technology, No. 79 West Yingze Street, Taiyuan 030024, People's Republic of China

[2] School of Nano-Science and Nano-Engineering, Suzhou & Collaborative Innovation Center of Suzhou Nano Science and Technology, Xi'an Jiaotong University, Xi'an 710049, People's Republic of China

[3] Center for Advanced Microstructures and Devices, Louisiana State University, Baton Rouge, LA 70806, USA

Introduction

Semiconductor metal oxides (SMOs) have attracted tremendous attention in chemical sensors due to the distinctive resistivity changing features in a certain ambient [1, 2]. As an *n*-type semiconductor, ZnO has been extensively used as a gas-sensing material due to its wide band gap (3.37 eV) and high exciton binding energy (60 meV) at room temperature [3–9]. Nevertheless, some inherent drawbacks including high operating temperature, slow response/recovery time, and low sensitivity may hinder the further development of ZnO-based gas sensors. So, great efforts have been made in the last decades to overcome the above-mentioned limitations using different methods, including noble metal doping, structure optimization, and heterostructure fabricating [10–12]. However, noble metal doping and heterostructure fabricating methods exist the problems of high cost as well as complex fabricating process. It seems that the morphologically controllable synthesis of ZnO nanomaterials is a feasible way for the improvement of the gas-sensing properties [11], because the gas-sensing is a surface-controlled process and influenced by the specific surface area.

Recently, hierarchical nanostructures including urchin-like, flower-like, and forest-like that derive from low-dimensional nanostructures (e.g., nanowires, nanorods, nanobelts, nanotubes, and nanofibers), have aroused a great deal of attention for the improvement of potential

gas-sensing performance [12–20]. For example, Yao et al. [18] obtained spherical ZnO nanobelt-flowers via pyrolysis process, the highly exposed surfaces of nanobelt branches provide high response of 6.94–44.1 ppm benzene gas. Hieu et al. [19] prepared urchin-like ZnO microspheres by sputtering Zn onto the template of a polystyrene sphere, and it shows a sensing of tens of ppb levels of NO concentrations with good response and gas selectivity. Yu et al. [20] synthesized micro-lotus ZnO nanosheets using a facile hydrothermal method, and the hierarchical structure presents excellent response towards ethanol and acetone. Among these hierarchical nanostructures, brush-like nanostructures assemblies of nanowires/rods are very attractive for fabricating efficient gas sensor, because the well-aligned morphology can augment the carrier transport and can be easily affected by the gas molecules [21–23]. Although considerable efforts have been devoted to improving gas-sensing performances using hierarchical nanostructures, there is seldom research work on synthesis brush-like ZnO homostructures for enhanced gas-sensing applications.

In this work, brush-like ZnO hierarchical nanostructures have been synthesized combining electrospinning and hydrothermal method. The brush-like ZnO nanowires and ZnO nanofibers gas sensors have been fabricated, and the gas-sensing properties were investigated for toluene and CO under the optimum working temperature. The measured results show that brush-like ZnO nanowires sensor exhibits enhanced gas-sensing performances comparing with ZnO nanofibers, which suggests that the brush-like ZnO nanowires are very promising materials for the application of gas sensors.

Experimental

Synthesis

All the reagents were of analytical grade and used without further purification. In a typical procedure, 0.50 g of zinc acetate dehydrate ($Zn(AC)_2{\cdot}2H_2O$) was dissolved into 2 mL *N*,*N*-dimethylformamide (DMF) to form transparent solution under vigorous stirring. Then, 0.25 g poly (vinyl pyrrolidone) (PVP, Mw = 1,300,000) was added into the above solution. The mixture was aged at room temperature for 4 h to obtain a homogeneous viscous sol solution as the precursor for electrospinning. The precursor solution was transferred into a 1-mL syringe with a hypodermic needle (inner diameter = 0.51 mm, 21*G*) in a home-made electrospinning equipment, and electrospun by applying 8 kV at an electrode distance of 12 cm at room temperature with a relative humidity (RH) of 37 %. The composite nanofibers were collected on an aluminum frame and peeled off from the frame. Finally, the crystal ZnO nanofibers were obtained after calcined at 600 °C for 2 h. In order to get brush-like ZnO nanowires, the as-prepared ZnO nanofibers were grown as our previous work [24]. Figure 1 illustrates the procedures for fabricating brush-like ZnO nanowires.

Characterization

The thermal behaviors of the samples were characterized using a thermal gravimetric analyzer (TGA, Melttler Toledo 825). Fourier transform infrared spectroscopy (FTIR, Bruker TENSOR 27) was introduced to characterize the samples using KBr pellets. The crystallographic information of the samples was investigated by X-ray powder diffraction (XRD, DRIGC-Y 2000A) using Cu $K\alpha_1$ radiation ($\lambda = 1.5406$ Å) as the radiation source. Morphology and structural investigations were observed using field emission scanning electron microscopy (FE-SEM, JEM-7100F) and transmission electron microscope (TEM, JEM-2100F). The specific surface area was measured using a surface area analyzer (Tristar 3020).

Fabrication and measurement of gas sensors

In a typical produce, the as-prepared ZnO nanostructures were mixed with moderate terpineol and ethyl cellulose with a weight ratio of 2:8:1 to form a homogeneous paste, which was coated onto a ceramic tube with a pair of Au electrodes and Pt wires for electrical contacts (Fig. 2a). Then, the elements were dried in air and annealed at 600 °C for 2 h. Finally, a Ni–Cr heating wire was inserted in the tube for controlling the working temperature by

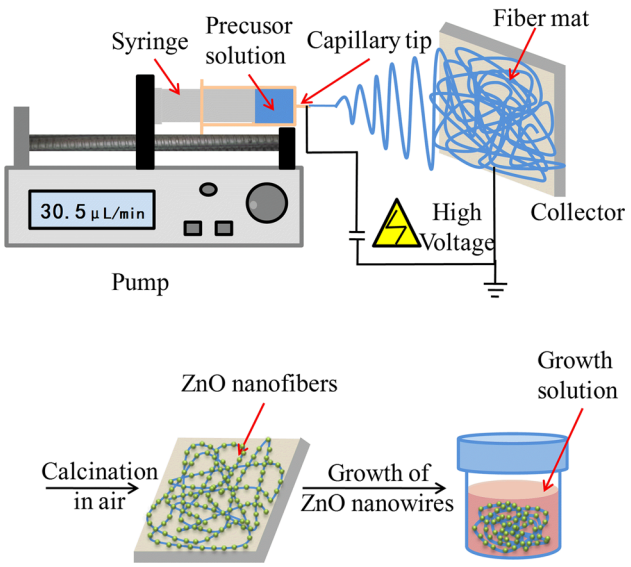

Fig. 1 Processing steps for the fabrication of brush-like ZnO nanowires combining electrospinning and hydrothermal method

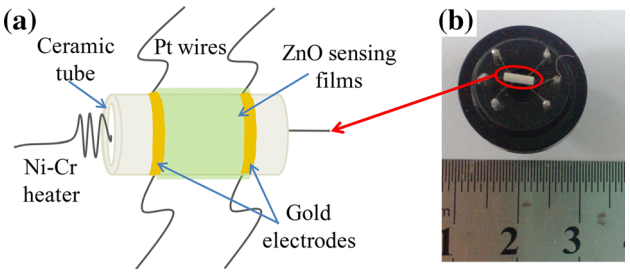

Fig. 2 **a** Schematic of ZnO sensing element, **b** photograph of the integrated sensor coated with the ZnO sensing materials

tuning the voltage. The alumina tube was welded onto a pedestal with six probes to give the final sensor unit, as shown in Fig. 2b. The gas-sensing properties of the sensors were measured by CGS-1TP intelligent analysis system (Elite, Beijing, China) using a static test system. The target vapor was injected into the test chamber (about 1 L in volume) by a syringe through a rubber plug. After fully mixed with air (RH was about 25 %), the sensor was put into the test chamber manually. When the response reached a constant value, the sensor was taken out of the chamber to recover in air. The sensor sensitivity (response) was defined as R_a/R_g, where R_a and R_g were the resistance of the sensor upon exposure to air and to the target gas. The time taken by the sensor to reach 90 % of the total resistance change was defined as the response and recovery time in the case of gas adsorption and desorption, respectively.

Results and discussion

Morphology and structure analysis

To obtain the ZnO nanofibers, $Zn(Ac)_2$/PVP composite nanofibers were calcined using muffle furnace. The thermal behaviors experiments were carried out on pure PVP nanofibers and $Zn(Ac)_2$/PVP composite nanofibers. Figure 3 shows the thermal events combustion process for $Zn(Ac)_2$/PVP composite nanofibers. The first process could be attributed to the loss of residual solvent and water remaining in the composite nanofibers from 100 to 270 °C [25, 26]. The second mass loss was ascribed to the complete degradation of PVP and the decomposition of acetates between 270 and 500 °C. Over 500 °C, the weights of the samples remain constant, which proves that all the volatiles and organic components are removed completely. The weight loss process of pure PVP nanofibers also contains three steps, which begins to occur at about 350 °C and completes at about 600 °C. Comparing with PVP nanofibers, the $Zn(Ac)_2$/PVP composite nanofibers has lower thermal stability. It can be attributed to the interaction between the PVP and ZnO materials. Based on the TGA

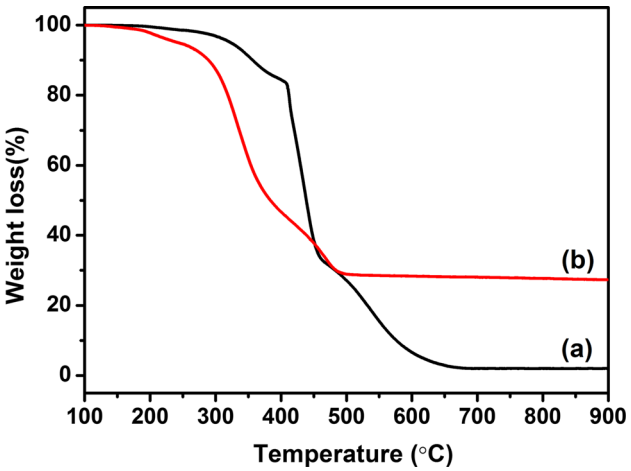

Fig. 3 TGA curves of *a* PVP nanofibers and *b* $Zn(Ac)_2$/PVP composite nanofibers

curves, the temperature of 600 °C was selected as the calcination temperature in the following procedure.

Figure 4 depicts the FTIR spectra of PVP nanofibers, $Zn(Ac)_2$/PVP composite nanofibers, ZnO nanofibers, and brush-like ZnO nanowires. It can be clearly seen that the FTIR spectra of PVP nanofibers and $Zn(Ac)_2$/PVP composite nanofibers possess strong peaks at around 1285, 1438, and 1661 cm^{-1} which are assigned to the C–C, C–H, and C=O stretching vibration of PVP [27]. The broad peak observed at 3280–3500 cm^{-1} comes from the water absorption [25]. However, for the spectra of ZnO nanofibers and brush-like ZnO nanowires, it is found that the characteristic peaks of PVP have disappeared because of the removal of the organic molecules. Simultaneously, a new peak is observed at around 475 cm^{-1} in the spectra of

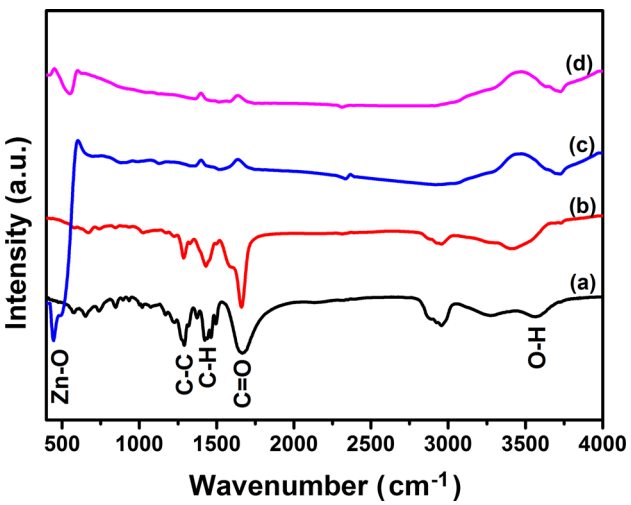

Fig. 4 FTIR spectra of various samples: *a* PVP nanofibers, *b* $Zn(Ac)_2$/PVP composite nanofibers, *c* ZnO nanofibers, and *d* brush-like ZnO nanowires

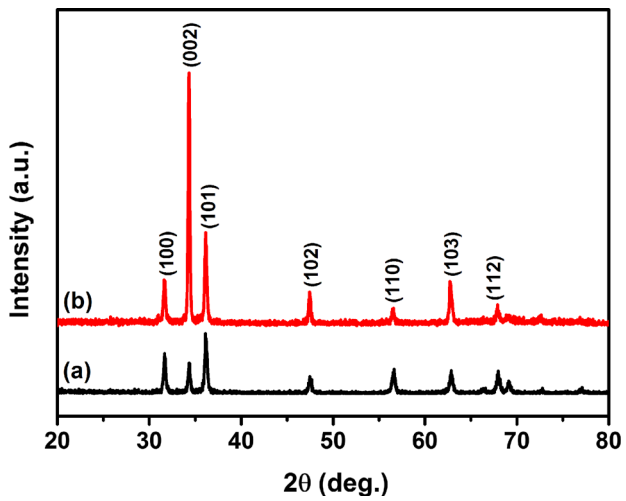

Fig. 5 XRD patterns of the obtained nanostructures: *a* ZnO nanofibers, *b* brush-like ZnO nanowires

ZnO nanofibers and brush-like ZnO nanowires, which can be attributed to the vibration of Zn–O bonds in ZnO crystals [13, 25].

Figure 5 shows the XRD diffraction patterns of ZnO nanofibers and brush-like ZnO nanowires. Both of the diffraction peaks are corresponding to hexagonal wurtzite structure of ZnO, which can be indexed with standard JCPDS data card no. 36-1451. There is no remarkable shift in diffraction peak, which indicates that no intermediate products are produced during the reaction. From the curve b, we can clearly find that the (002) peak is much stronger and sharper for brush-like ZnO nanowires, which indicates the high-quality crystallinity and *c* axis orientation.

Figure 6a reveals the SEM images of the ZnO nanofibers after calcination, which displays a randomly distributed and interweaved to form a network. The amplified inset image shows that the diameter is about 160 nm for the single nanofiber, and the BET surface area of the ZnO nanofibers can reach to 2.892 m^2g^{-1}. At the same time, the detail morphology characterization of ZnO nanofibers is performed using TEM. Figure 6b shows the low-resolution TEM image of ZnO nanofibers, it is found that the nanofibers were composed of plenty of nanoparticles with sizes around 25–35 nm. Figure 6c illustrates the typical high-resolution TEM (HRTEM) image, and the measured lattice spacing values of 0.26 nm is corresponding to the ZnO (0001) plane [10, 28]. Figure 6d exhibits the selected area electron diffraction (SAED) pattern, which can be attributable to the fact that the ZnO nanofibers are polycrystalline.

The brush-like ZnO nanostructures were obtained by hydrothermal growth, which is built up from compactly aggregated, irregular-shaped ZnO nanowires (Fig. 7a). From the high-magnification SEM image (inset), we can clearly observe that the nanowires attach vertically to the sidewall of nanofibers with a length of 3 μm. Figure 7b presents the brush-like ZnO nanowires with a low magnification, and ZnO nanowires are uniformly distributed on the surface of nanofibers. Figure 7c exhibits the typical HRTEM image of ZnO nanowires. The lattice fringes between two adjacent planes are about 0.52 nm which is equal to the lattice constant of the ZnO. The measured results demonstrate that the ZnO nanowires grow along the [0001] direction [9, 29], and the corresponding SAED pattern proves that the ZnO nanowires are single crystals (Fig. 7d). Moreover, the measured BET surface area of the brush-like ZnO nanowires can reach to 5.982 m^2g^{-1}, which is twice as big as ZnO nanofibers.

Sensing performance and mechanism

Due to its unique hierarchical structures, brush-like ZnO nanowires can provide an advantage for gas-sensing applications. Therefore, we fabricated chemical gas sensors based on ZnO nanofibers and brush-like ZnO nanowires,

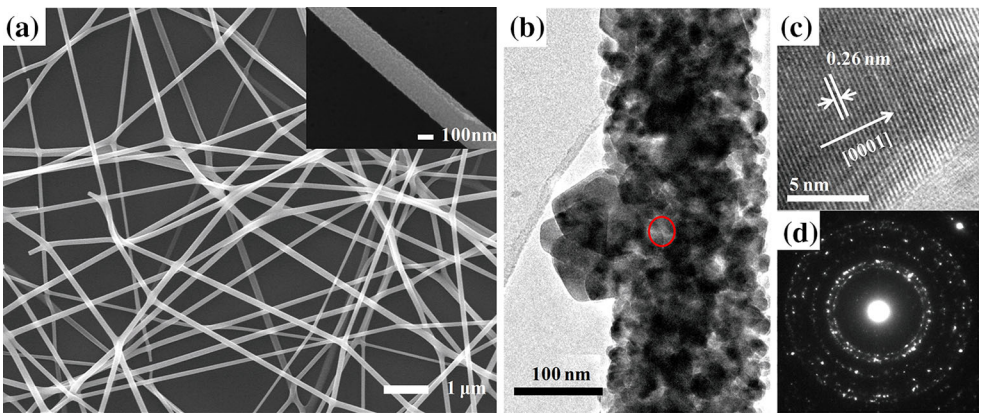

Fig. 6 The ZnO nanofibers, **a** SEM image, **b** TEM image, **c** HRTEM image, and **d** corresponding SAED pattern

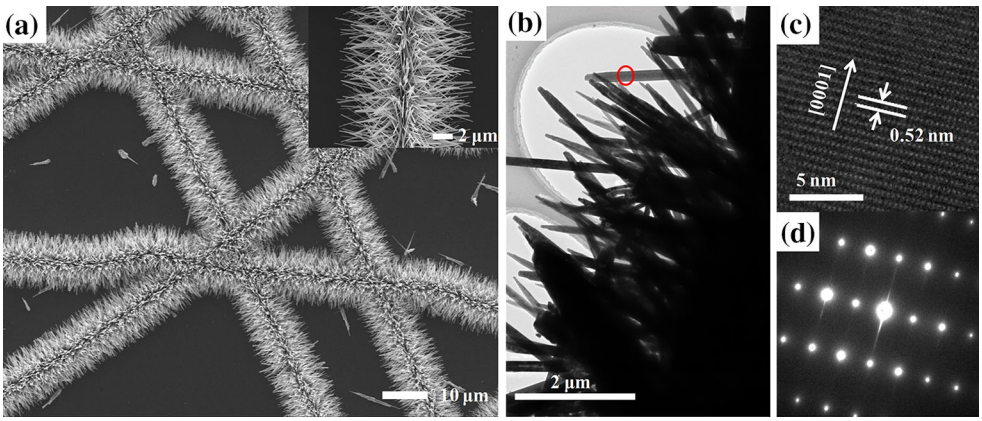

Fig. 7 The brush-like ZnO nanowires, **a** SEM image, **b** TEM image, **c** HRTEM image, and **d** corresponding SAED pattern

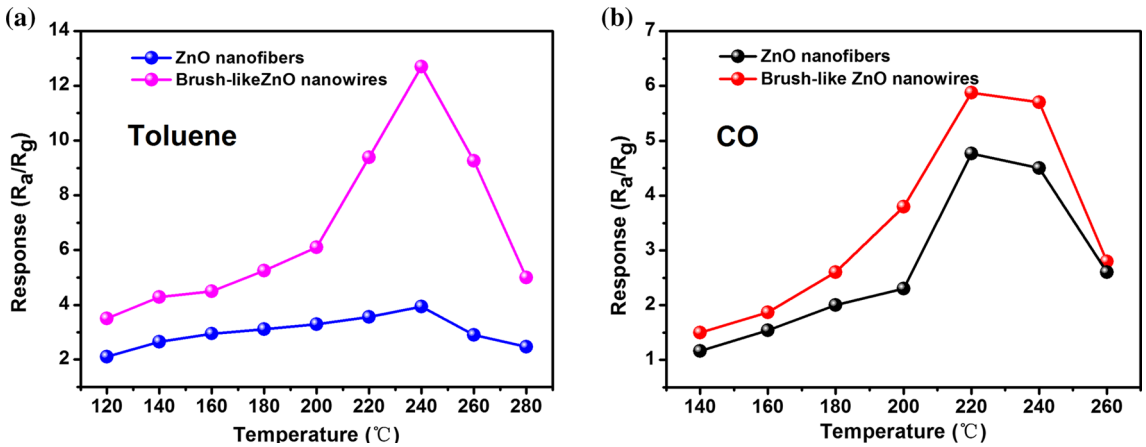

Fig. 8 Relationship between working temperature and response of the as-prepared sensors under 100 ppm, **a** toluene, **b** CO

and then compared their gas-sensing performance for toluene and CO detection.

In order to optimize the working temperature, gas-sensing experiments were conducted on the as-prepared gas sensors. Figure 8a shows the response of ZnO nanofibers and brush-like ZnO nanowires sensors to 100 ppm toluene under the working temperature between 120 and 280 °C. The responses of both ZnO nanofibers and brush-like ZnO nanowires gas sensors all increase slowly and reach their maximum at 240 °C, and then decreases with increasing the temperature further. The decrease of response can be attributed to that some adsorbed test gas molecules easily escape from the surface of ZnO before their reaction since the working temperature is too high [11, 30]. At the optimum temperature of 240 °C, brush-like ZnO nanowires exhibit the highest response of about 12.7 to toluene, which is 3.3 times larger than that of ZnO nanofibers. Moreover, the similar tendency can be also observed for the CO under different working temperatures as Fig. 8b. Under the optimum working temperature (220 °C), the response of brush-like ZnO nanowires to CO can reach to 5.9, which is about 1.25-folds higher than that of ZnO nanofibers.

Figure 9 shows the sensing transient of as-fabricated sensors to toluene and CO with different concentrations under their optimum temperatures. From Fig. 9a, b, we can clearly observe that both ZnO nanofibers and brush-like ZnO nanowires gas sensors show a clear and fast response increases with increasing the concentration of toluene and CO. After many cycles between exposure to detection gas and fresh air, the resistances of the sensors can recover to their initial values, which suggest that all the fabricated sensors have good reversibility and distinguished reproducibility. In addition, the brush-like ZnO nanowires sensor exhibits a higher response under the same gas concentration compared with ZnO nanofibers sensor, which is about twofold to sixfold enhancement. However, there is no remarkable enhancement for CO, when the gas concentrations are under 100 ppm. At the same time, in order to confirm the relationships between response and gas concentrations, the sensitivities of fabricated sensors are plotted as a function of the gas concentration as Fig. 9c, d.

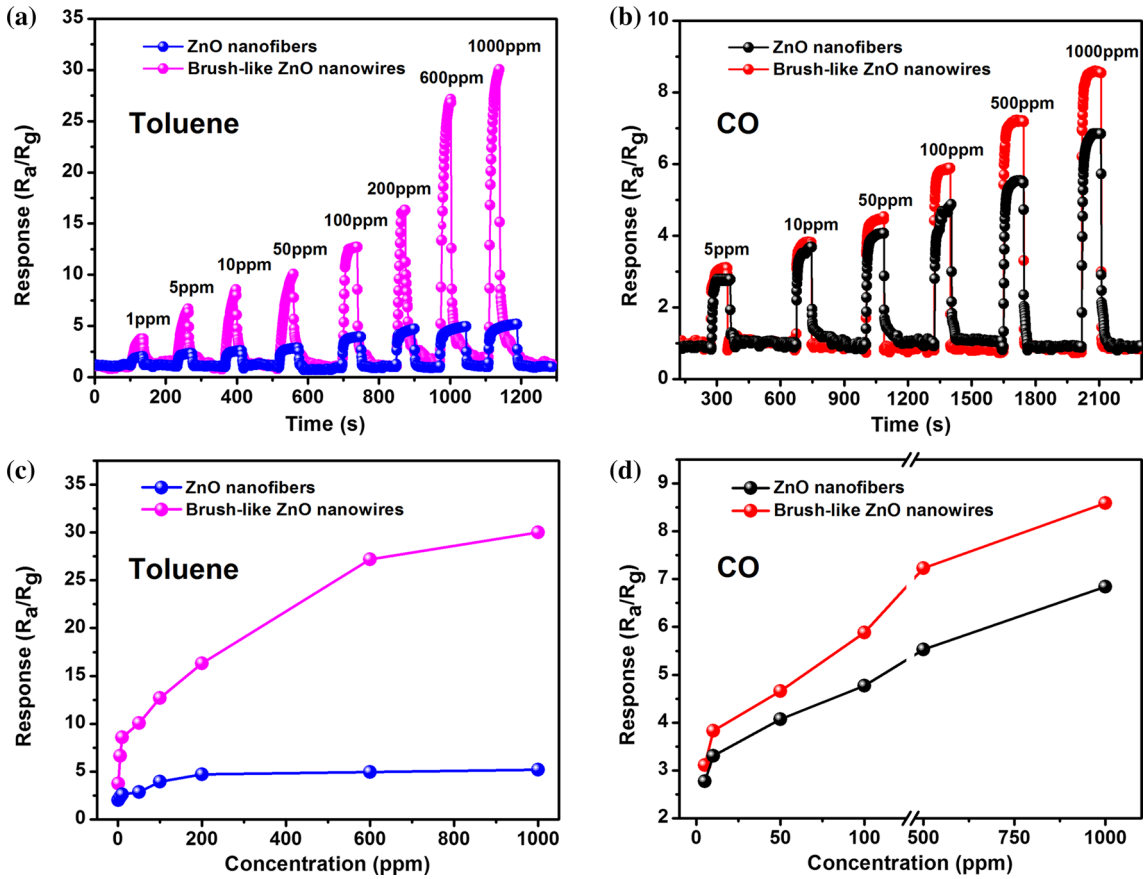

Fig. 9 Dynamic sensing transients of the ZnO nanofibers and brush-like ZnO nanowires sensors; **a** toluene, **b** CO; The dependence of the sensors response, **c** toluene, **d** CO

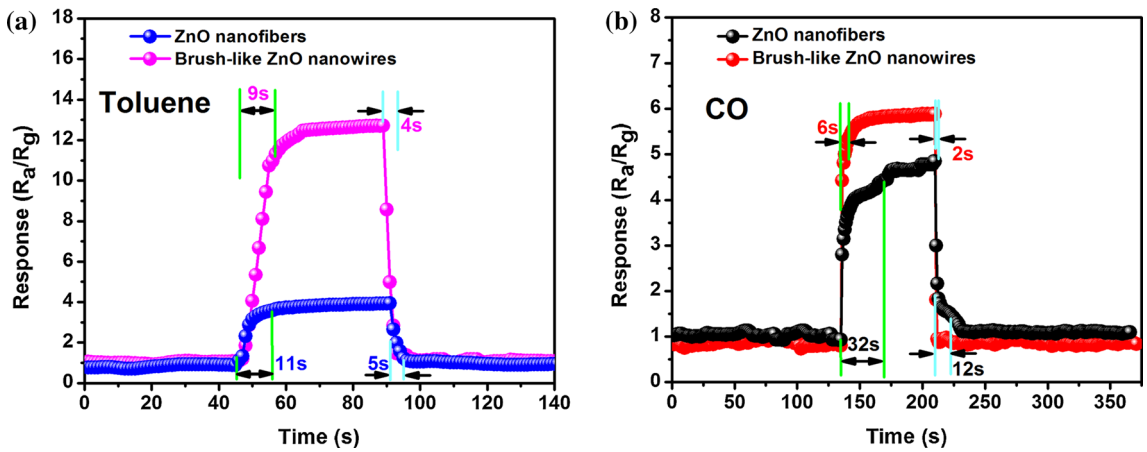

Fig. 10 Response and recovery behavior of sensors to100 ppm. **a** toluene, **b** CO

The measured results exhibit that the fabricated gas sensors tend to reach saturation states at high gas concentration for toluene and CO. Moreover, the brush-like ZnO nanowires sensor displays improvement response for toluene, and the detection limit for brush-like ZnO nanowires can down to 1 ppm for toluene and 5 ppm for CO with the responses of 3.8 and 3.2, respectively.

Response and recovery characteristics are the main parameters in design of gas sensors for desired applications. Figure 10 shows the magnified response/recovery

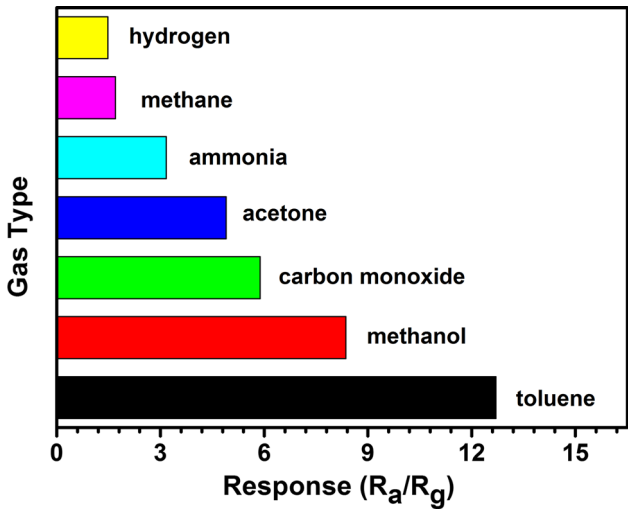

Fig. 11 Response of brush-like ZnO nanowires sensor to different kinds of gases for 100 ppm at 240 °C

plots for toluene and CO with the concentration of 100 ppm. The measured response/recovery times of brush-like ZnO nanowires sensor are just 9/4 s and 6/2 s for toluene and CO, respectively, which are much shorter than that of ZnO nanofibers sensor (11/5 s for toluene and 32/12 s for CO). From the measured results, we can find that the brush-like ZnO nanowires sensor has faster response/recovery speed comparing with ZnO nanowires sensor.

For a gas sensor, gas selectivity is another important parameter in practical applications. Therefore, the responses of brush-like ZnO nanowires sensor to 100 ppm methanol, carbon monoxide, acetone, ammonia, methane, and hydrogen are also investigated under the optimized working temperature of 240 °C (Fig. 11). It is obvious that the brush-like ZnO nanowires sensor exhibits higher response to toluene than to other tested gases, and there are no apparent response to methane and hydrogen. Nevertheless, further investigation may still be required to improve the selectivity of the material via surface modification and bulk doping with heteroatom for methanol and carbon monoxide. At the same time, to compare the sensing performances of the fabricated brush-like ZnO nanowires gas sensor, we summarized the previous reported ZnO-based toluene gas sensor in Table 1 [31–36]. From the measured results, we can find that the fabricated brush-like ZnO nanowires gas sensor has higher sensitivity, faster response/recovery time, and lower working temperature.

The excellent sensing capabilities observed in the brush-like ZnO nanowires sensor are likely to be associated to the hierarchical structures, which exhibits unique loose structures and high surface area [37]. The brush-like ZnO nanowires possess much higher specific surface area than that of the ZnO nanofibers. Compared with ZnO nanofibers, when exposed to the target gas, the hierarchical brush-like structures with a number of branch structures can increase the surface area to absorb more target gas and

Table 1 Gas-sensing properties comparison of toluene gas sensors based on various structures of ZnO in the literatures and in this study

Sample	Toluene (ppm)	Response	t_{res}/t_{rec} (s)	T (°C)	Reference
ZnO nanowire	100	6.43	–/–	340	[31]
Au–ZnO NWs	100	36	36/45	350	[32]
Porous ZnO nanowire	100	~28	–/–	300	[33]
Flower-like ZnO nanorods	100	7.4	7/10	390	[34]
Flower-like ZnO structures	100	2.3	15/55	240	[35]
Porous single-crystalline ZnO nanosheets	100	~3	5/40	220	[36]
Brush-like ZnO nanowires	**100**	**12.7**	**9/4**	**240**	**This work**

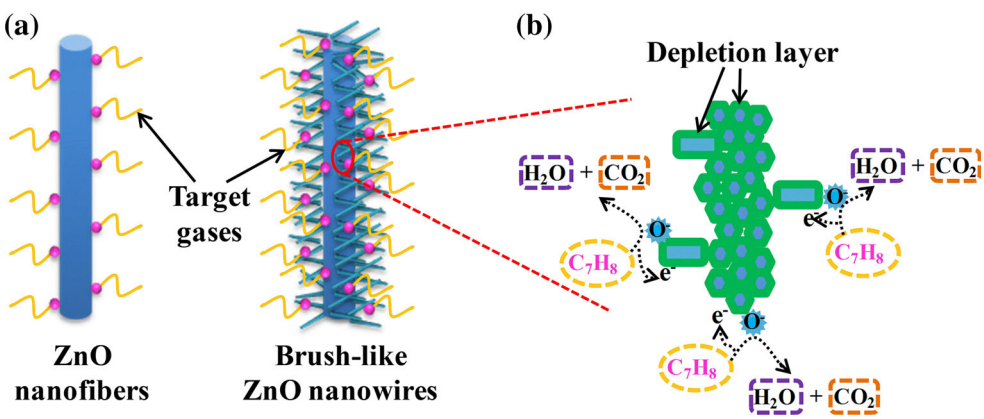

Fig. 12 **a** Schematic illustrations of hierarchical structures sensing mechanism, **b** schematic diagram of catalytic reactions

provide more active sites for the interaction with the gas as in Fig. 12a, and the adsorbed oxygen ions will interact with the target gas to produce CO_2 and H_2O (Fig. 12b). At the same time, larger amount of electrons will release into the conduction band of ZnO, leading to the lower resistance and higher response of the sensor. Furthermore, the gas diffusion speed and length are significant factors that affect the response and recovery time of ZnO gas sensors [30]. ZnO nanowires are generally assembled in highly periodic, thus there is no impediment in gas diffusion towards the entire sensing surface, resulting in fast response and recovery time. As a consequence, the gas-sensing performance of brush-like ZnO nanowires is greatly improved.

Conclusions

In summary, the brush-like ZnO nanowires was synthesized by two-step method combining electrospinning and hydrothermal. The unique brush-like ZnO hierarchical structures are composed of the ZnO nanowires branches which are uniformly deposited on the surface of ZnO nanofibers. In order to investigate the gas-sensing characteristics, two types of sensors were prepared for the detection of toluene and CO. The experiments results show that the response of brush-like ZnO nanowires sensor can reach to 12.7 and 5.9 for toluene and CO under the optimum temperature, which is much higher than that of ZnO nanofibers sensor. Moreover, brush-like ZnO nanowires sensor also exhibits fast response/recovery times for toluene (9/4 s) and CO (6/2 s), which are much shorter than that of ZnO nanofibers sensor (11/5 s for toluene and 32/12 s for CO). These measured results suggest that brush-like ZnO nanowires can be a promising material structure for the application high-performance gas sensors.

Acknowledgements The authors gratefully acknowledge the financial support of the National Natural Science Foundation of China (Grant Nos. 51205274 and 51205276), the Shanxi Province Science Foundation for Youths (Grant No. 2013021017-2), the Shanxi Scholarship Council of China (Grant No. 2013-035), Doctoral Fund of Ministry of Education of China (Grant No. 20121402120008), China Postdoctoral Science Foundation (Grant No. 2013M530894), Graduate Education Innovation Fund (Grant No. 02100738), Technology Foundation for Selected Overseas Shanxi Scholar ([2014] 95), Science and Technology Major Project of the Shanxi Science and Technology Department (Grant No. 20121101004), and Key Disciplines Construction in Colleges and Universities of Shanxi (Grant No. [2012] 45).

References

1. Lee JH (2009) Gas sensors using hierarchical and hollow oxide nanostructures: overview. Sens Actuators B 140:319–336
2. Choi SJ, Choi CY, Kim SJ, Cho HJ, Hakim M, Jeon S, Kim D (2015) Highly efficient electronic sensitization of non-oxidized graphene flakes on controlled pore-loaded WO_3 nanofibers for selective detection of H_2S molecules. Sci Rep-uk. doi:10.1038/srep08067
3. Liang YC, Liao WK, Deng XS (2014) Synthesis and substantially enhanced gas sensing sensitivity of homogeneously nanoscale Pd- and Au-particle decorated ZnO nanostructures. J Alloy Compd 599:87–92
4. Gardon M, Guilemany JM (2013) A review on fabrication, sensing mechanisms and performance of metal oxide gas sensors. J Mater Sci 24:1410–1421. doi:10.1007/s10854-012-0974-4
5. Hu J, Gao FQ, Sang SB, Li PW, Deng X, Zhang WD, Chen Y, Lian K (2015) Optimization of Pd content in ZnO microstructures for high-performance gas detection. J Mater Sci 50:1935–1942. doi:10.1007/s10853-014-8758-2
6. Wang WC, Tian YT, Wang XC, He H, Xu YR, He C, Li XJ (2013) Ethanol sensing properties of porous ZnO spheres via hydrothermal route. J Mater Sci 48:3232–3238. doi:10.1007/s10853-012-7103-x
7. Khoang ND, Hong HS, Trung DD, Duy NV, Hoa ND, Thinh DD, Hieu NV (2013) On-chip growth of wafer-scale planar-type ZnO nanorod sensors for effective detection of CO gas. Sens Actuators B 181:529–536
8. Zhang WH, Zhang WD, Zhou JF (2010) Solvent thermal synthesis and gas-sensing properties of Fe-doped ZnO. J Mater Sci 45:209–215. doi:10.1007/s10853-009-3920-y
9. Luo J, Ma SY, Li FM, Li XB, Li WQ, Cheng L, Mao YZ, GZ DJ (2014) The mesoscopic structure of flower-like ZnO nanorods for acetone detection. Mater Lett 121:137–140
10. Song N, Fan HQ, Tian HL (2015) PVP assisted in situ synthesis of functionalized graphene/ZnO (FGZnO) nanohybrids with enhanced gas-sensing property. J Mater Sci 50:2229–2238. doi:10.1007/s10853-014-8785-z
11. Tarwal NL, Rajgure AV, Patil JY, Khandekar MS, Suryavanshi SS, Patil PS, Gang MG, Kim JH, Jang JH (2013) A selective ethanol gas sensor based on spray-derived Ag–ZnO thin films. J Mater Sci 48:7274–7282. doi:10.1007/s10853-013-7547-7
12. Zhang ZY, Li XH, Wang CH, Wei LM, Liu YC, Shao CL (2009) ZnO hollow nanofibers: fabrication from facile single capillary electrospinning and applications in gas sensors. J Chem Phys C 113:19397–19403
13. Zhang XJ, Qiao GJ (2012) High performance ethanol sensing films fabricated from ZnO and In_2O_3 nanofibers with a double-layer structure. Appl Surf Sci 258:6643–6647
14. Xu J, Yu YS, He XX, Sun JB, Liu FM, Lu GY (2012) Synthesis of hierarchical ZnO orientation-ordered film by chemical bath deposition and its gas sensing properties. Mater Lett 81:145–147
15. Meng F, Yin J, Duan YQ, Yuan ZH, Bie LJ (2011) Co-precipitation synthesis and gas-sensing properties of ZnO hollow sphere with porous shell. Sens Actuators B 156:703–708
16. Shafiei M, Yu J, Chen G, Lai PT, Motta N, Wlodarski W, Kalantar-zadeh K (2013) Improving the hydrogen gas sensing performance of Pt/MoO_3 nanoplatelets using a nano thick layer of La_2O_3. Sens Actuators B 187:267–273
17. Wei YL, Huang YF, Wu JH, Wang M, Guo CS, Dong Q (2013) Synthesis of hierarchically structured ZnO spheres by facile methods and their photocatalytic de NO_x properties. J Hazard Mater 248:202–210
18. Yao MS, Hu P, Cao YB, Xiang WC, Zhang X, Yuan FL, Chen YF (2013) Morphology-controlled ZnO spherical nanobelt-flower arrays and their sensing properties. Sens Actuators B 177:562–569
19. Hieu HN, Yuong NM, Jung H, Jang DM, Kim D, Kim H, Hong S (2012) Optimization of a zinc oxide urchin-like structure for high-performance gas sensing. J Mater Chem 3:1127–1134

20. Yu A, Qian JS, Pan H, Cui YM, Xu MG, Tu L, Chai QL, Zhou XF (2011) Micro-lotus constructed by Fe-doped ZnO hierarchically porous nanosheets: preparation, characterization and gas sensing property. Sens Actuators B 158:9–16
21. Lou Z, Li F, Deng JN, Wang LL, Zhang T (2013) Branch-like hierarchical heterostructure (α-Fe_2O_3/TiO_2): a novel sensing material for trimethylamine gas sensor. Appl Mater Interface 5:12310–12316
22. Zhang Y, Xu JQ, Xiang Q, Li H, Pan QY, Xu PC (2009) Brush-like hierarchical ZnO nanostructures: synthesis, photoluminescence and gas sensor properties. J Phys Chem C 113:3430–3435
23. Rakshit T, Santra S, Manna I, Ray SK (2014) Enhanced sensitivity and selectivity of brush-like SnO_2 nanowire/ZnO nanorod heterostructure based sensors for volatile organic compounds. RSC Adv 4:36749–36756
24. Hu J, Sun YJ, Zhang WD, Gao FQ, Li PW, Jiang D, Chen Y (2014) Fabrication of hierarchical structures with ZnO nanowires on micropillars by UV soft imprinting and hydrothermal growth for a controlled morphology and wettability. Appl Surf Sci 317:545–551
25. Khorami HA, Rad MK, Vaezi MR (2011) Synthesis of SnO_2/ZnO composite nanofibers by electrospinning method and study of its ethanol sensing properties. Appl Surf Sci 257:7988–7992
26. Mali SS, Kim H, Jang WY, Park HS, Patil PS, Hong CK (2013) Novel synthesis and characterization of mesoporous ZnO nanofibers by electrospinning technique. ACS Sustain Chem Eng 1:1207–1213
27. Park SJ, Chase GG, Jeong K, Kim HY (2010) Mechanical properties of titania nanofiber mats fabricated by electrospinning of sol–gel precursor. J Sol-Gel Sci Technol 54:188–194
28. Kushwaha A, Aslam M (2014) ZnS shielded ZnO nanowire photoanodes for efficient water splitting. Electrochim Acta 130:222–231
29. Guo T, Luo YD, Zhang YJ, Lin YH, Nan CW (2014) Controllable growth of ZnO nanorod arrays on NiO nanowires and their high UV photoresponse current. Cryst Growth Des 14:2329–2334
30. Liu L, Li SC, Zhang J, Wang LY, Zhang JB, Li HY, Liu Z, Han Y, Jiang XX, Zhang P (2011) Improved selective acetone sensing properties of Co-doped ZnO nanofibers by electrospinning. Sens Actuators B 155:782–788
31. Tang W, Wang J (2015) Mechanism for toluene detection of flower-like ZnO sensors prepared by hydrothermal approach: charge transfer. Sens Actuators B 207:66–73
32. Wang LW, Wang SR, Xu MJ, Hu XJ, Zhang HX, Wang YH, Huang WP (2013) A Au-functionalized ZnO nanowire gas sensor for detection of benzene and toluene. Phys Chem Chem Phys 15:17179–17186
33. Zeng Y, Zhang T, Wang LJ, Kang MH, Fan HT, Wang R, He Y (2009) Enhanced toluene sensing characteristics of TiO_2-doped flowerlike ZnO nanostructures. Sens Actuators B 140:73–78
34. Hjiri M, Mir LE, Leonardi SG, Pistone A, Mavilia L, Neri G (2014) Al-doped ZnO for highly sensitive CO gas sensors. Sens Actuators B 196:413–420
35. Zhang HJ, Wu RF, Chen ZW, Liu G, Zhang ZN, Jiao Z (2012) Self-assembly fabrication of 3D flower-like ZnO hierarchical nanostructures and their gas sensing properties. CrystEngComm 14:1775–1782
36. Huang JE, Ren HB, Sun PP, Gu CP, Sun YF, Liu JH (2013) Facile synthesis of porous ZnO nanowires consisting of ordered nanocrystallites and their enhanced gas-sensing property. Sens Actuators B 188:249–256
37. Deng JN, Yu B, Lou Z, Wang LL, Wang R, Zhang T (2013) Facile synthesis and enhanced ethanol sensing properties of the brush-like ZnO-TiO_2 heterojunctions nanofibers. Sens Actuators B 184:21–26